International Conference on Automation, Control Engineering and Computer Science (ACECS)
Proceedings of Engineering and Technology – PET
Vol.20 pp.25 - 28

Nonlinear Control of Single-Phase Grid Connected PV Generator through Multicellular Inverter

Taghzaoui Chaimaa[#1], Abouloifa Abdelmajid[#2], Lachkar Ibtissam[*3],
Elallali Aicha[#4], Hamdoun Abdelatif[#5]

[#] *LTI Lab, University HASSAN II of Casablanca, Faculty of Science Ben M'sik, CO 7955 Casablanca, Morocco*
[1]taghzaouichaimaa@gmail.com
[2]abouloifa@yahoo.fr
[4]aichaelallali@gmail.com
[5]alhamdoun@yahoo.fr
[*]*LRI Lab, University HASSAN II of Casablanca, ENSEM Casablanca, CO 7955 Casablanca, Morocco*
[3]lachkaribtissam@gmail.com

Abstract— **A nonlinear control methodology for single-phase grid connected of photovoltaic generator is presented in this paper. It consists of a PV arrays, a voltage source Multicellular inverter, a grid filter and an electric grid. The controller objectives are threefold: i) ensuring the Maximum power point tracking (MPPT) in the side of PV panels, ii) guaranteeing a power factor unit in the side of the grid, iii) ensuring a good convergence of the voltages across the flying capacitors. On the basis of the nonlinear model of the entire system, the controller is carried out using an approach of Lyapunov. The simulation results have been performed through Matlab/Simulink environment and show that the designed controller meets its objective.**

Keywords— **single-phase PV grid-connected inverters; nonlinear control, MPPT; Backstepping approach; Lyapunov stability.**

I. Introduction

The world energy supply is still dominated by fossil fuels. In fact, according to recent published statistics [1], these resources constitute more than 80% of total primary energy. Power generation based on fossil-fuel combustion releases about 10 billion tons of carbon emissions per year and thus contributes to climate change with severe and irreversible consequences on the environment. Therefore, ensuring a secure and sustainable energy supply is one of the most important challenges facing the world, especially with the population growth and the improvement of living standards [2-3]. In this respect, photovoltaic (PV) based renewable energy presents several features e.g. simplicity of allocation, high dependability, absence of fuel cost, low maintenance and lack of noise and wear due to the absence of moving parts. In addition to these benefits, the recent progress made in the PV technology has resulted in quite lower cost and more efficient PV cells. This evolution is expected to continue in the future due to economies scale [4-6]. A comprehensive discussion about single-phase grid connected PV system with power conditioning capability has been given in [7,8]. Multilevel converters are proper alternatives for medium and high power applications and possess some advantages like increased number of output voltage levels, which improves output voltage spectrum with low harmonic distortion and reduces filter requirements.

In this work the flying capacitor multicellular (FCM) converter [9].is the only power converter interfacing the PV generator and single-phase grid, (see Fig. 1). This simpler structure prevents the disadvantages of using chopper (additional losses, investment and maintenance).

Several strategies for control have been proposed in the literature in order to improve the characterization of this topology for example: sliding modes in [10- 12] hybrid control in [13-15] predictive control in [16-19] and passivity based control in [20].

The rest of the paper is organized as follows: in section 2, the description and the modeling of the system are presented, sections 3 is devoted to the controller design and the controller performances are illustrated through simulations under MATLAB/Simulink software in Section 4.

II. System Description And Modeling

A. System description

The main circuit of single phase grid-connected photovoltaic system is shown in Fig.1. It consists of a PV arrays; two DC link capacitor C_1 and C_2; a single phase inverter (including 3 elementary switching cells in series, each switching cell of the converter is composed of pairs of complementary switches); a LCL filter is used in order to minimize the harmonics distortion of current and voltage and an electric grid.

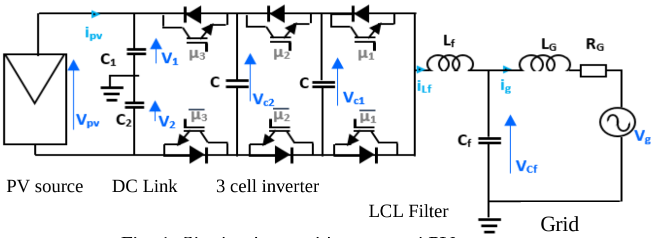

Fig. 1 Single-phase grid connected PV system

As there is no DC-DC converter between the PV generator and the inverter, the PV array configuration should be chosen such that the output voltage of the photovoltaic generator is adapted to the requirements of the inverter, so the inverter would need at least 780V DC bus in order to be able to operate

ISSN 2356-5608

correctly. The PV array was found to require 22 series connected modules per string. Each solar module has the following Electrical specifications: Maximum Power P_m=200 W, Short circuit current I_{sc}=8.21 A, Open circuit voltage V_{oc}=32.9 V, Maximum power voltage V_m=26.3 V, Maximum power current I_m=7.61 A.

B. Converter and filter modeling

Applying Kirchhoff's laws, the system under study is described by the following set of differential equations:

$$L_g\ \dot{i}_g = v_c - v_g - r\ i_g \quad (1.a)$$

$$C_f\ \dot{v}_c = i_{Lf} - i_g \quad (1.b)$$

$$L_f\ \dot{i}_{Lf} = (\mu_1 - \mu_2)\, v_{c1} + (\mu_2 - \mu_3)\ v_{c2} + \mu_3\ v_1 - v_c \quad (1.c)$$

$$C\ \dot{v}_{c1} = (\mu_2 - \mu_1)\, i_{Lf} \quad (1.d)$$

$$C\,\dot{v}_{c2} = (\mu_3 - \mu_2)\, i_{Lf} \quad (1.e)$$

$$C_1\ \dot{v}_1 = i_{pv} - \mu_1\ i_{Lf} \quad (1.f)$$

$$C_2\ \dot{v}_2 = i_{pv} - (1 - \mu_1)\, i_{Lf} \quad (1.g)$$

where $\mu_i \in \{0,1\}, i = 1,2,3$.

The model (1a-c) However, it cannot used in the control design as it involves a binary control input, namely μ. For control design purpose, it is more convenient to consider the following averaged model:

$$L_g\ \dot{x}_1 = x_2 - v_g - r_g\ x_1 \quad (2.a)$$

$$C_f\ \dot{x}_2 = x_3 - x_1 \quad (2.b)$$

$$L_f\ \dot{x}_3 = (u_1 - u_2)\, x_4 + (u_2 - u_3)\ x_5 + u_3\ x_6 - x_2 \quad (2.c)$$

$$C\ \dot{x}_4 = (u_2 - u_1)\, x_3 \quad (2.d)$$

$$C\ \dot{x}_5 = (u_3 - u_2)\, x_3 \quad (2.e)$$

$$C_1\ \dot{x}_6 = i_{pv} - u_1\ x_3 \quad (2.f)$$

$$C_2\ \dot{x}_7 = i_{pv} - (1 - u_1)\, x_3 \quad (2.g)$$

where $x_1, x_2, x_3, x_4, x_5, x_6$ and u_i denote the average values, over cutting periods, of the signals i_g, v_c, i_{Lf}, v_{c1}, v_{c2}, v_1, and μ_i.

III. Controller Design

A. Control objectives

The control objectives can be formulated as follows:

i) ensuring the (MPPT) in the side of PV panels, the controller must enforce the average value of the voltage $x_7 = \bar{V}_{pv}$ provided by the solar array to track as possible a given desired value of the reference voltage $x_7 = V_{pv}^*$.

ii) guaranteeing a power factor unit in the side of the grid, by injecting (in the grid) a current with sinusoidal shape and in phase with a grid voltage, $x_1 = \beta V_g$ (3)

iii) ensuring a good convergence of the voltages across the flying capacitors at its desired reference values:

$$x_3^* = \frac{V_{pv}^*}{3} \quad (5) \qquad \text{and} \qquad x_4^* = \frac{2V_{pv}^*}{3} \quad (4)$$

B. Nonlinear control design

Following the backstepping technique, the controller is designed in tree steps.

- **Step 1:**

Let us define the following tracking error:

$$z_1 = C\left(x_4 - x_4^*\right) \quad (5.a)$$

$$z_2 = C\left(x_5 - x_5^*\right) \quad (5.b)$$

$$z_3 = L_g\ \left(x_1 - x_1^*\right) \quad (5.c)$$

with x_5^*, x_4^* and x_1^* represent respectively the desired trajectories of x_5, x_4 and x_1.

Deriving z_1, z_2 and z_3 with respect to time yields and accounting for (1a) and (1c-d), implies:

$$\dot{z}_1 = (u_2 - u_1)\, x_3 - C\ \dot{x}_4^* \quad (6.a)$$

$$\dot{z}_2 = (u_3 - u_2) x_3 - C\ \dot{x}_5^* \quad (6.b)$$

$$\dot{z}_3 = x_2 - v_g - r_g\ x_1 - L_g\ \dot{x}_1^* \quad (6.c)$$

We need to select a Lyapunov function for such system. As the objective is to drive its state (z_1, z_2, z_3) to zero, it is natural to choose the following function:

$$V_1 = 0.5\, z_1^2 + 0.5\, z_2^2 + 0.5 z_3^2 \quad (7.a)$$

Its time derivative is given by the following equation:

$$\dot{V}_1 = z_1\, \dot{z}_1 + z_2\, \dot{z}_2 + z_3\, \dot{z}_3 \quad (7.b)$$

The choice $\dot{V}_1 = -\lambda_1\, z_1^2 - \lambda_2\, z_2^2 - \lambda_3\, z_3^2$, where $\lambda_i (i = 1,\ldots,3)$ are positive constants of synthesis, leads to a Lyapunov candidate function whose dynamics is negative definite.

In view of (7b) and using (6) this suggests the following choices:

$$(u_2 - u_1)\, x_3 - C\ \dot{x}_4^* = -\lambda_1\ z_1 \quad (8.a)$$

$$(u_3 - u_2)\, x_3 - C\ \dot{x}_5^* = -\lambda_2\ z_2 \quad (8.b)$$

$$x_2 - v_g - r_g\ x_1 - L_g\ \dot{x}_1^* = -\lambda_3\ z_3 \quad (8.c)$$

if we choose x_2 as virtual control input, we deduce the stabilizing function namely x_2^*:

$$x_2^* = -\lambda_3\ z_3 + v_g + r_g\ x_1 + L_g\ \dot{x}_1^* \quad (9)$$

as x_2 is not the control input, a new error variable z_4 between x_2 and its desired value x_2^* is introduced:

$$z_4 = C_f\ \left(x_2 - x_2^*\right) \quad (10)$$

using (10) and (9) , dynamics of error z_3 became:

$$\dot{z}_3 = \frac{z_4}{C_f} - \lambda_3\ z_3 \quad (11)$$

In the same way

$$\dot{V}_1 = -\lambda_1\, z_1^2 - \lambda_2\, z_2^2 - \lambda_3\, z_3^2 + \frac{z_3\ z_4}{C_f} \quad (12)$$

- **Step 2:**

ISSN 2356-5608

The objective now is to enforce the error variables (z_1, z_2, z_3, z_4) to vanish. To this end, let us first determine the dynamics of z_4 , we obtain:

$$\dot{z}_4 = x_3 - x_1 - C_f \dot{x}_2^* \qquad (13)$$

Consider the augmented Lyapunov function candidate.

$$V_2 = V_1 + 0.5 z_4^2 \qquad (14.a)$$

Using(12)-(14.a) ,its dynamics is given by:

$$\dot{V}_2 = -\lambda_1 z_1^2 - \lambda_2 z_2^2 - \lambda_3 z_3^2 + z_4 \left(\frac{z_3}{C_f} + \dot{z}_4 \right) \qquad (14.b)$$

As our goal is to make $\dot{V}_2$ non-positive definite $\dot{V}_2 = -\lambda_1 z_1^2 - \lambda_2 z_2^2 - \lambda_3 z_3^2 - \lambda_4 z_4^2 \leq 0$, this suggests choosing that the bracketed term, in (14.C), is equal to $-\lambda_4 z_4$:

$$\dot{z}_4 = -\lambda_4 z_4 - \frac{z_3}{C_f} \qquad (15)$$

where λ_4 is a positive constant of synthesis. if we choose x_3 as virtual control input, we deduce the stabilizing function namely x_3^* :

$$x_3^* = x_1 + C_f \dot{x}_2^* - \lambda_4 z_4 - \frac{z_3}{C_f} \qquad (16)$$

As x_3 is not the control input, a new error variable z_5 between x_3 and its desired value x_3^* is introduced:

$$z_5 = L_f \left(x_3 - x_3^* \right) \qquad (17)$$

using (11) and (16) , dynamics of error z_4 became:

$$\dot{z}_4 = \frac{z_5}{L_f} - \lambda_4 z_4 - \frac{z_3}{C_f} \qquad (18)$$

In the same way

$$\dot{V}_2 = -\lambda_1 z_1^2 - \lambda_2 z_2^2 - \lambda_3 z_3^2 - \lambda_4 z_4^2 + \frac{z_4 z_5}{L_f} \qquad (19)$$

- **Step 3:**

The objective now is to enforce the error variables to vanish. To this end, let us determine the dynamics of z_5 , we obtain:

$$\dot{z}_5 = (u_1 - u_2) x_4 + (u_2 - u_3) x_5 + u_3 x_6 - x_2 - L_f \dot{x}_3 \qquad (20)$$

We are finally in a position to make a convenient choice of the parameter update law and feedback control to stabilize the whole system with state vector $(z_1, z_2, z_3, z_4, z_5)$,Consider the augmented Lyapunov function candidate.

$$V_3 = V_2 + 0.5 z_5^2 \qquad (21.a)$$

Using (19)-(21.a) ,its dynamics is given by:

$$\dot{V}_3 = -\lambda_1 z_1^2 - \lambda_2 z_2^2 - \lambda_3 z_3^2 - \lambda_4 z_4^2 + z_5 \left(\frac{z_4}{L_f} + \dot{z}_5 \right) \qquad (21.c)$$

As our goal is to make $\dot{V}_3$ non-positive definite $\dot{V}_3 = -\lambda_1 z_1^2 - \lambda_2 z_2^2 - \lambda_3 z_3^2 - \lambda_4 z_4^2 - \lambda_5 z_5^2 \leq 0$, this suggests choosing that the bracketed term, on the right side of (21c), is equal to $-\lambda_5 z_5$:

$$\dot{z}_5 = -\lambda_5 z_5 - \frac{z_4}{L_f} \qquad (22)$$

Finally, the control input can be solved from the following system equations.

$$u_3 = \frac{f_1}{x_6} \text{ where } \begin{aligned} f_1 = &(u_2 - u_1) x_4 + (u_3 - u_2) x_5 + L_f \dot{x}_3^* \\ &+ x_2 - \frac{C_f \left(x_2 - x_2^* \right)}{L_f} - \lambda_5 L_f \left(x_3 - x_3^* \right) \end{aligned} \qquad (23)$$

$$u_2 = u_3 - \frac{C \dot{x}_5^* - \lambda_2 C \left(x_5 - x_5^* \right)}{x_3} \qquad (24)$$

$$u_1 = u_2 - \frac{C \dot{x}_4^* - \lambda_1 C \left(x_4 - x_4^* \right)}{x_3} \qquad (25)$$

where λ_5 is a positive constant of synthesis.

C. MPPT Controller Design

Maximum power point tracking, or MPPT, is the automatic adjustment of the load of a photovoltaic system to achieve the maximum possible power output. The output of the PV cells is expressed as the current-voltage characteristic of the PV cell. The maximum power point tracking (MPPT) can be addressed by different ways, in this paper we worked with the algorithm perturb and observe (P&O) which is the most method used due to its simplicity and a fewer measured parameter, it has two input signals. The algorithm steps are described as shown in the following flowchart (Fig.3). [21]

IV. Simulation Results

The proposed control scheme, presented in Fig. 4, is validated through simulations performed using the Matlab/Simulink and its SimPower SystemToolbox.

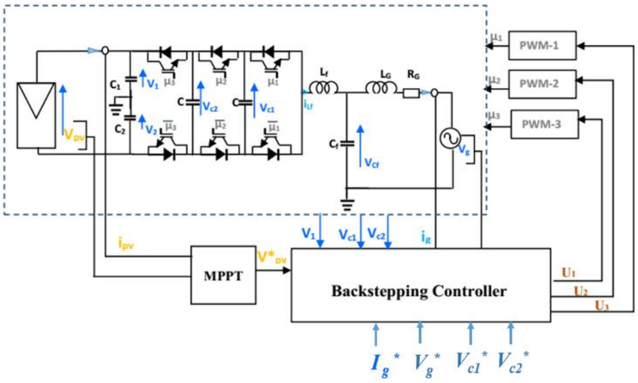

Fig. 4 Control block for multicellular inverter

The proposed control scheme, presented in Fig. 4 is validated through simulations performed using the Matlab/Simulink environment. The simulation results have been obtained under standard climatic conditions (λ=1000 W/m² and T=25°C) with the following parameters: Flying capacitor C and Dc link capacitors C_2=C_1=4 mF Filter capacitor C_f=5 mF, Filter inductor L_f=2 mH and grid inductors L_g=30 mH, R_g=35 Ω
The control design parameter are given: λ_1=400, λ_2=200, λ_3=20000, λ_4=200 ,λ_5=900, $\beta = 10 / \left(220 * \sqrt{2} \right)$ and the Switching frequency f_s =10 kHz.

ISSN 2356-5608

The resulting control performances are shown by Fig 5 to 8. Fig. 5 shows the PV voltage with its reference generated by the "P&O" algorithm. The voltage of the PV array V_{pv} after 0.18s varies between V_{pv}=600V and V_{pv}=700V and then returns to 780V, which correspond very well to the optimum voltage.

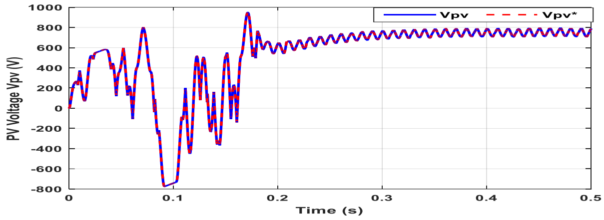

Fig. 5 PV voltage with its reference

The capacitor voltages v_{c1} and v_{c2} shown in Fig (6-7) converge towards their desired values, after 0.21 seconds they reach the reference voltages. Fig 8 shows that the current i_g and the grid voltage V_g are sinusoidal and in phase, As a result, a unit power factor is achieved.

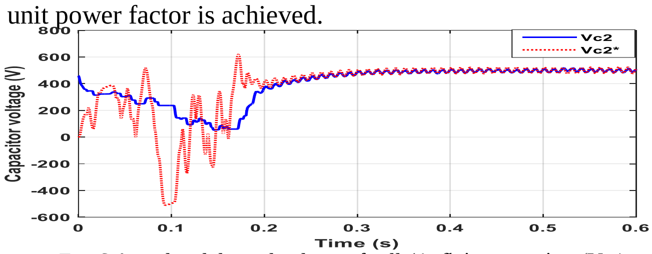

Fig. 6 Actual and desired voltage of cell-1's flying capacitor (V_{C1})

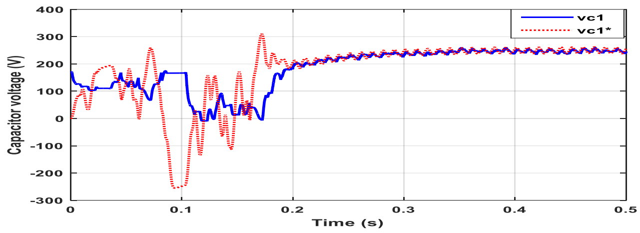

Fig. 7 Actual and desired voltage of cell-2's flying capacitor (V_{c2})

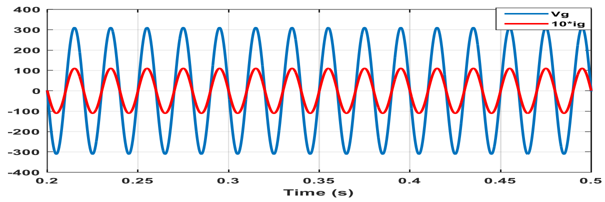

Fig.8 Unity PF behavior

V. Conclusions

In this paper an advanced controller is developed for PV grid connected system. The latter is described by 5[th] order nonlinear averaged model. The controller design is made based on backstepping technique and Lyapunov stability. Simulations under Matlab/Simulink prove that the controller meet the performances, for which it was designed, namely: i) Global asymptotic stability of the all system ii) Perfect power factor in the grid iii) Maximum power point tracking.

References

[1] (2015) International Energy Agency (IEA), Energy and Climate Change, World Energy Outlook Special Report,<www.iea.org>.

[2] A. Allouhi, Y. El Fouih, T. Kousksou, A.Jamil, Y. Zeraouli, and Y. Mourad, "Energy consumption and efficiency in buildings: current status and future trends," *Journal of Cleaner Production.*, vol. 109, pp.118-130, 2015.

[3] P. Novak, "Sustainable energy system with zero emissions of GHG for cities and countries, " *Energy and Buildings.*, vol. 98, pp. 27-33, 2015

[4] JM. Pacas, MG. Molina, Jr .EC. dos Santos, "Design of a robust and efficient power electronic interface for the grid integration of solar photovoltaic generation Systems," *Int J Hydrogen Energy*, vol 37,pp. 10076–82, 2012.

[5] N. Caglayan, C. Ertekin, F. Evrendilek, "Spatial viability analysis of grid-connected photovoltaic power systems for Turkey," *Int J Electr Power Energy Syst*, vol. 56(3), pp. 270–8, 2014.

[6] A. El Fadili, F. Giri, and A. El Magri, "Reference voltage optimizer for maximum power point tracking in triphase grid-connected photovoltaic systems," *International Journal of Electrical Power & Energy Systems*, vol. 60, pp. 293-301, 2014.

[7] R. A. Mastromauro, M. Liserre, A. Dell'Aquila, "Single phase grid-connected photovoltaic systems with power quality conditioner functionality," *IEEE European Conference on Power Electronics and Applications,Alborg, Denmark*, pp. 1-11. 2007.

[8] R. A. Mastromauro, M. Liserre, T. Kerekes, A. Dell'Aquila, "A single-phase voltage-controlled grid-connected photovoltaic system with power quality conditioner functionality," *IEEE Transactions on Industrial Electronics*,vol. 56, pp. 4436-4444, 2009.

[9] A. K. Sadigh, S. H. Hosseini, M. Sabahi, G. B. Gharehpetian, "Double flying capacitor multicell converter based on modified phase-shift pulse width modulation," *IEEE Transactions on Power Electronics*, vol. 25, pp.1517-1526, Aug 2010.

[10] C. Morvan, P.Y. Richard, H. Cormerais, J. Buisson, "Sliding mode control of switching systems with Boolean inputs," in *IFAC Conference NOLCOS, Stuttgart*, pp.747-752, September 2004.

[11] M. Djemaï, K. Busawon, K. Benmansour, A. Marouf, "High-Order Sliding Mode Control of a DC Motor Drive via a Switched Controlled Multi-Cellular Converter," *International Journal of Systems Science*, Vol. 42, pp. 1869-1882, 2011..

[12] L. Amet, M. Ghanes, and J. P Barbot. "Direct control based on sliding mode techniques for multicell serial chopper," *American Control Conference (ACC)*, pp. 751– 756, 2011.

[13] S. Elmetennani ,T.M. Laleg-Kirati , M. Djemai and M. Tadjine , "New MPPT algorithm for PV applications based on hybrid dynamical approach," *Journal of Process Control*, Vol. 48, pp. 14–24 ,Dec 2016.

[14] M. Benmiloud, A. Benalia, "Finite-time stabilization of the limit cycle of two-cell DC/DC converter: hybrid approach," *Nonlinear Dyn*, vol. 83, pp. 319–332, 2016.

[15] M. Benmiloud, A. Benalia, M. Defoort, M. Djemaï, "On the limit cycle stabilization of a DC/DC three-cell converter," Control *Engineering Practice*, Vol. 49, pp. 29-41, April 2016.

[16] D. Patino, M. Bâja, P. Riedinger, H. Cormerais, J. Buisson, and C. Iung, "Alternative control methods for DC–DC converters: an application to a four-level three-cell DC–DC converter," *International Journal of Robust and Nonlinear Control*, Vol 21(10), pp.1112–1133, 2011.

[17] D Patino, P. Riedinger, and C. Iung, "Predictive control approach for multilevel converters," *In Proceedings of the 34th annual conference of IEEE on industrial electronics, IECON*, pp. 1–6,2008.

[18] F. Defay, A. Llor, and M. Fadel, "A Predictive Control with Flying Capacitor Balancing of a Multicell Active Power Filter," *IEEE TRANSACTIONS ON INDUSTRIAL ELECTRONICS*, vol. 55(9), pp. 3212-3220, 2008.

[19] F. Defay, A. Llor, and M. Fadel, "An active power filter using a sensorless muticell inverter," *in Proc. IEEE ISIE*, pp. 679–684, 2007.

[20] H. Cormerais, J. Buisson, P.Y. Richard, and C .Morvan, "Modelling and passivity based control of switched systems from bond graph formalism: application to multicellular converters," *Journal of the Franklin Institute*, Vol 345(5), pp.68–488, 2008.

[21] B. Bhandari, S. Poudel, L. Kyung-Tae, and A. Sung-Hoon, "Mathematical Modeling of Hybrid Renewable Energy System: A Review on Small Hydro-Solar-Wind Power Generation," *International Journal of Precision Engineering and Manufacturing Green Technology*, Vol 1(2), pp. 157-173, 2014.

ISSN 2356-5608